

A Trilateral Weighted Sparse Coding Scheme for Real-World Image Denoising

Jun Xu¹, Lei Zhang¹, David Zhang^{1,2}

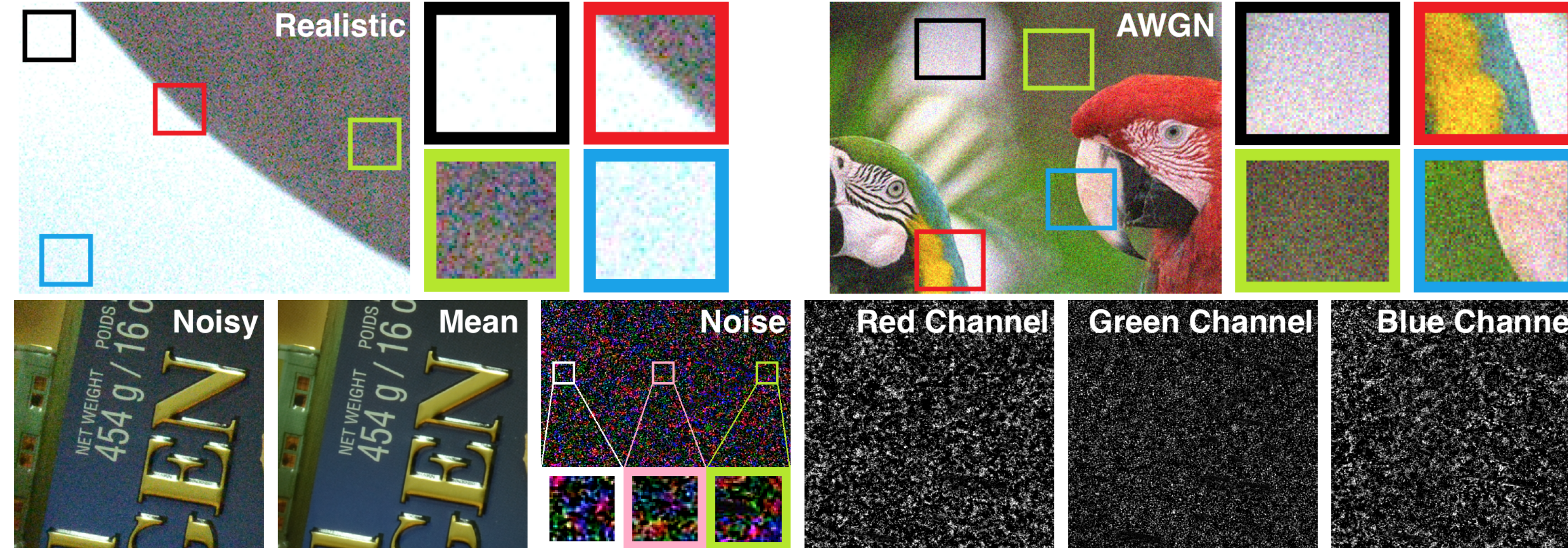
¹ Department of Computing, Hong Kong Polytechnic University, Hong Kong SAR, China

² School of Science and Engineering, The Chinese University of Hong Kong (Shenzhen), Shenzhen, China

Problem, Motivation, and Contributions

Goal: Estimating the latent clean image from the input real-world noisy image.

Motivation: Realistic noise show channel-wise and locally signal dependent property.



Contributions:

- Propose a trilateral weighted sparse coding (TWSC) scheme for real-world denoising;
- TWSC achieves much better performance than state-of-the-art denoising methods.

The TWSC Scheme

TWSC: Given a color image patch $\mathbf{Y} = \mathbf{X} + \mathbf{N} \in 3p^2 \times N$ and $\mathbf{Y} = \mathbf{DSV}^\top$ is the SVD of \mathbf{Y} . The TWSC model can be written as

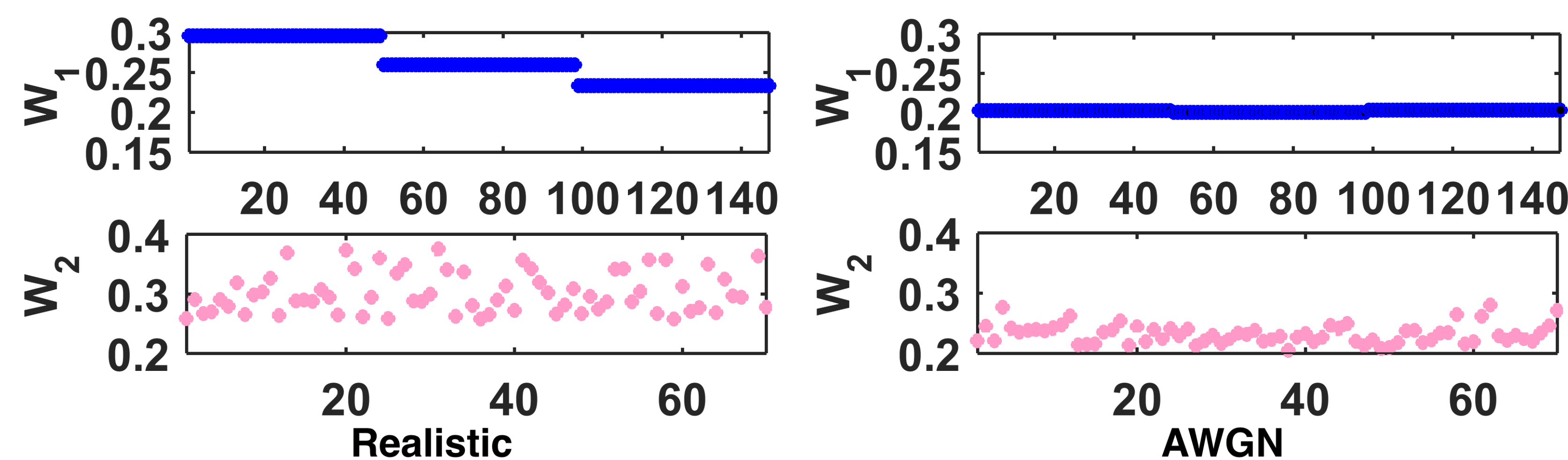
$$\hat{\mathbf{C}} = \arg \min_{\mathbf{C}} \|\mathbf{W}_1(\mathbf{Y} - \mathbf{DC})\mathbf{W}_2\|_F^2 + \|\mathbf{W}_3^{-1}\mathbf{C}\|_1. \quad (1)$$

The estimation of \mathbf{X} can be $\hat{\mathbf{X}} = \mathbf{DC}$.

Formulation of weight matrices:

$$\begin{aligned} \mathbf{W}_1 &= \text{diag}(\sigma_r^{-1/2}\mathbf{I}_{p^2}, \sigma_g^{-1/2}\mathbf{I}_{p^2}, \sigma_b^{-1/2}\mathbf{I}_{p^2}), \\ \mathbf{W}_2 &= \text{diag}(\sigma_1^{-1/2}, \dots, \sigma_M^{-1/2}), \mathbf{W}_3 = \mathbf{S}, \end{aligned} \quad (2)$$

Visualization of weight matrices:



Optimization

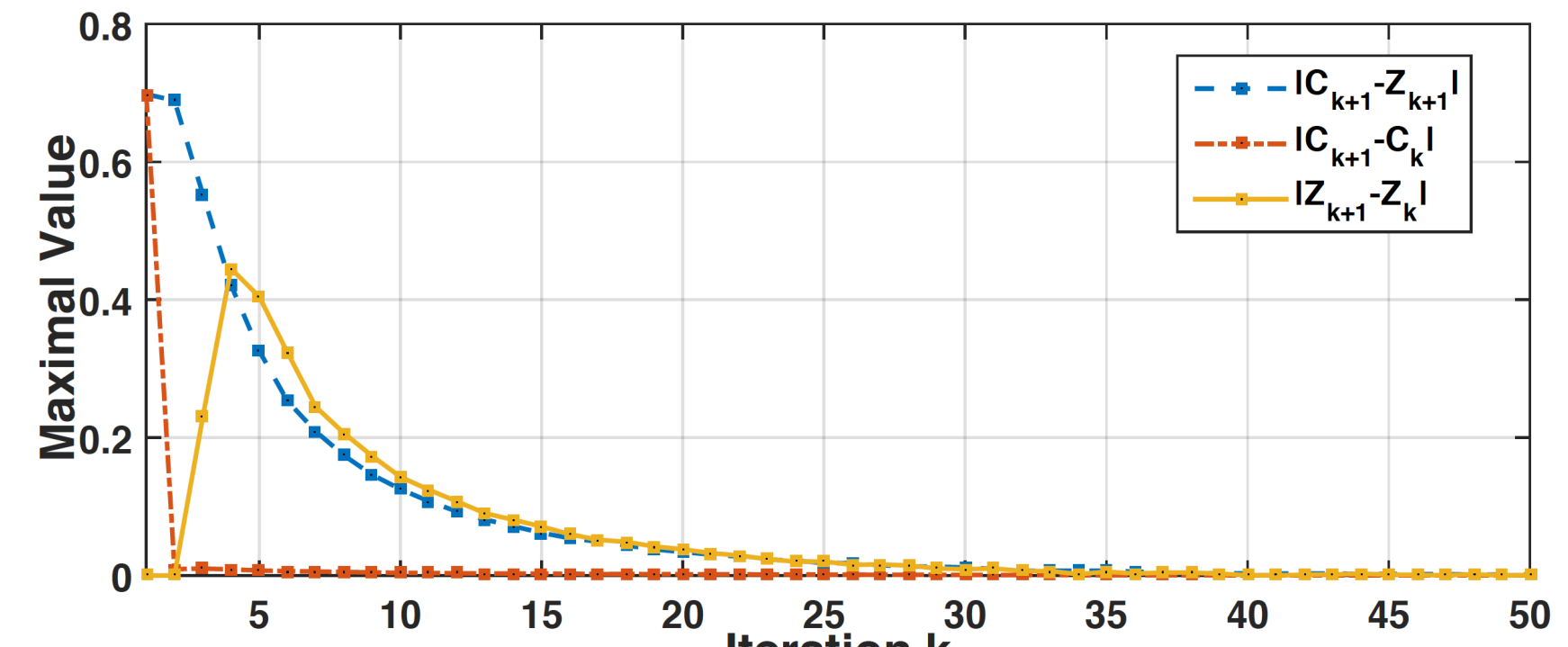
Variable Splitting: $\min_{\mathbf{C}, \mathbf{Z}} \|\mathbf{W}_1(\mathbf{Y} - \mathbf{DW}_3\mathbf{C})\mathbf{W}_2\|_F^2 + \|\mathbf{Z}\|_1$ s.t. $\mathbf{C} = \mathbf{Z}$.

ADMM:

- $\mathbf{C}_{k+1} = \arg \min_{\mathbf{C}} \|\mathbf{W}_1(\mathbf{Y} - \mathbf{DW}_3\mathbf{C})\mathbf{W}_2\|_F^2 + \frac{\rho_k}{2} \|\mathbf{C} - \mathbf{Z}_k + \rho_k^{-1}\Delta_k\|_F^2$.
The solution \mathbf{C}_{k+1} satisfies $\mathbf{AC}_{k+1} + \mathbf{C}_{k+1}\mathbf{B}_k = \mathbf{E}_k$, where $\mathbf{A} = \mathbf{W}_3^\top \mathbf{D}^\top \mathbf{W}_1^\top \mathbf{W}_1 \mathbf{D} \mathbf{W}_3$, $\mathbf{B}_k = \frac{\rho_k}{2} (\mathbf{W}_2 \mathbf{W}_2^\top)^{-1}$, $\mathbf{E}_k = \mathbf{W}_3^\top \mathbf{D}^\top \mathbf{W}_1^\top \mathbf{W}_1 \mathbf{Y} + (\frac{\rho_k}{2} \mathbf{Z}_k - \frac{1}{2} \Delta_k) (\mathbf{W}_2 \mathbf{W}_2^\top)^{-1}$.
(Solution) $\mathbf{C}_{k+1} = \text{vec}^{-1}((\mathbf{I}_M \otimes \mathbf{A} + \mathbf{B}_k^\top \otimes \mathbf{I}_{3p^2})^{-1} \text{vec}(\mathbf{E}_k))$.
Challenge: Is $(\mathbf{I}_M \otimes \mathbf{A} + \mathbf{B}_k^\top \otimes \mathbf{I}_{3p^2})^{-1}$ exist?
- $\mathbf{Z}_{k+1} = \arg \min_{\mathbf{Z}} \frac{\rho_k}{2} \|\mathbf{Z} - (\mathbf{C}_{k+1} + \rho_k^{-1} \Delta_k)\|_F^2 + \|\mathbf{Z}\|_1$.
- $\Delta_{k+1} = \Delta_k + \rho_k (\mathbf{C}_{k+1} - \mathbf{Z}_{k+1})$.
- $\rho_{k+1} = \mu \rho_k$, where $\mu \geq 1$.

Theoretical Analysis

Convergence:



Existence of the Solution to ADMM (a):

Theorem 1. Assume that $\mathbf{A} \in \mathbb{R}^{3p^2 \times 3p^2}$, $\mathbf{B} \in \mathbb{R}^{M \times M}$ are both symmetric and positive semi-definite matrices. If at least one of \mathbf{A} , \mathbf{B} is positive definite, the Sylvester equation $\mathbf{AC} + \mathbf{CB} = \mathbf{E}$ has a unique solution for $\mathbf{C} \in \mathbb{R}^{3p^2 \times M}$.

Corollary 1. The *Solution* to ADMM (a) exists and is unique.

Experimental Results

Quantitative Comparisons on AWGN Removal:

Table 1: Average results of PSNR(dB) and SSIM of different denoising algorithms on 20 grayscale images corrupted by AWGN noise.

σ_n	Metric	BM3D-SAPCA	LSSC	NCSR	WNNM	TNRD	DnCNN	WSC	TWSC
15	PSNR	32.42	32.27	32.19	32.43	32.27	32.59	32.06	32.34
	SSIM	0.8860	0.8849	0.8814	0.8841	0.8815	0.8879	0.8673	0.8846
25	PSNR	30.02	29.84	29.76	30.05	29.87	30.22	29.57	29.98
	SSIM	0.8364	0.8329	0.8293	0.8365	0.8314	0.8415	0.8179	0.8372
35	PSNR	28.48	28.26	28.17	28.51	28.33	28.66	28.01	28.49
	SSIM	0.7969	0.7908	0.7855	0.7958	0.7907	0.8021	0.7765	0.7987
50	PSNR	26.85	26.64	26.55	26.92	26.75	27.08	26.35	26.93
	SSIM	0.7481	0.7405	0.7391	0.7499	0.7415	0.7563	0.7258	0.7530
75	PSNR	24.74	24.77	24.66	25.15	24.97	25.24	24.54	25.15
	SSIM	0.6649	0.6746	0.6793	0.6903	0.6801	0.6931	0.6612	0.6949

Quantitative Comparisons on Realistic Noise Removal:

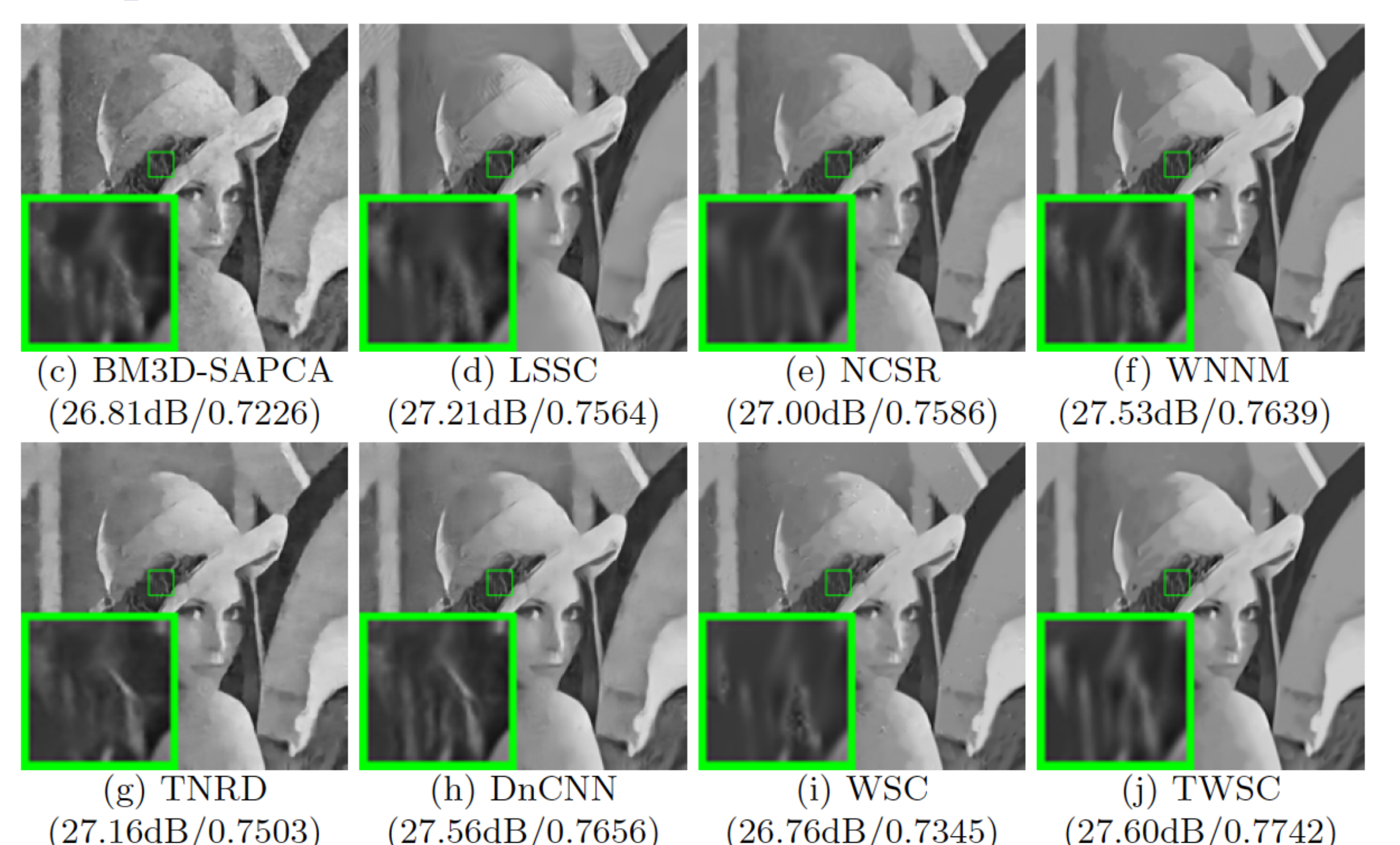
Table 2: Average results of PSNR(dB) and SSIM of different denoising methods on 15 cropped real-world noisy images used in [24].

	CBM3D	TNRD	DnCNN	NI	NC	CC	MCWNNM	WSC	TWSC
PSNR	35.19	36.61	33.86	35.49	36.43	36.88	37.70	37.36	37.81
SSIM	0.8580	0.9463	0.8635	0.9126	0.9364	0.9481	0.9542	0.9516	0.9586

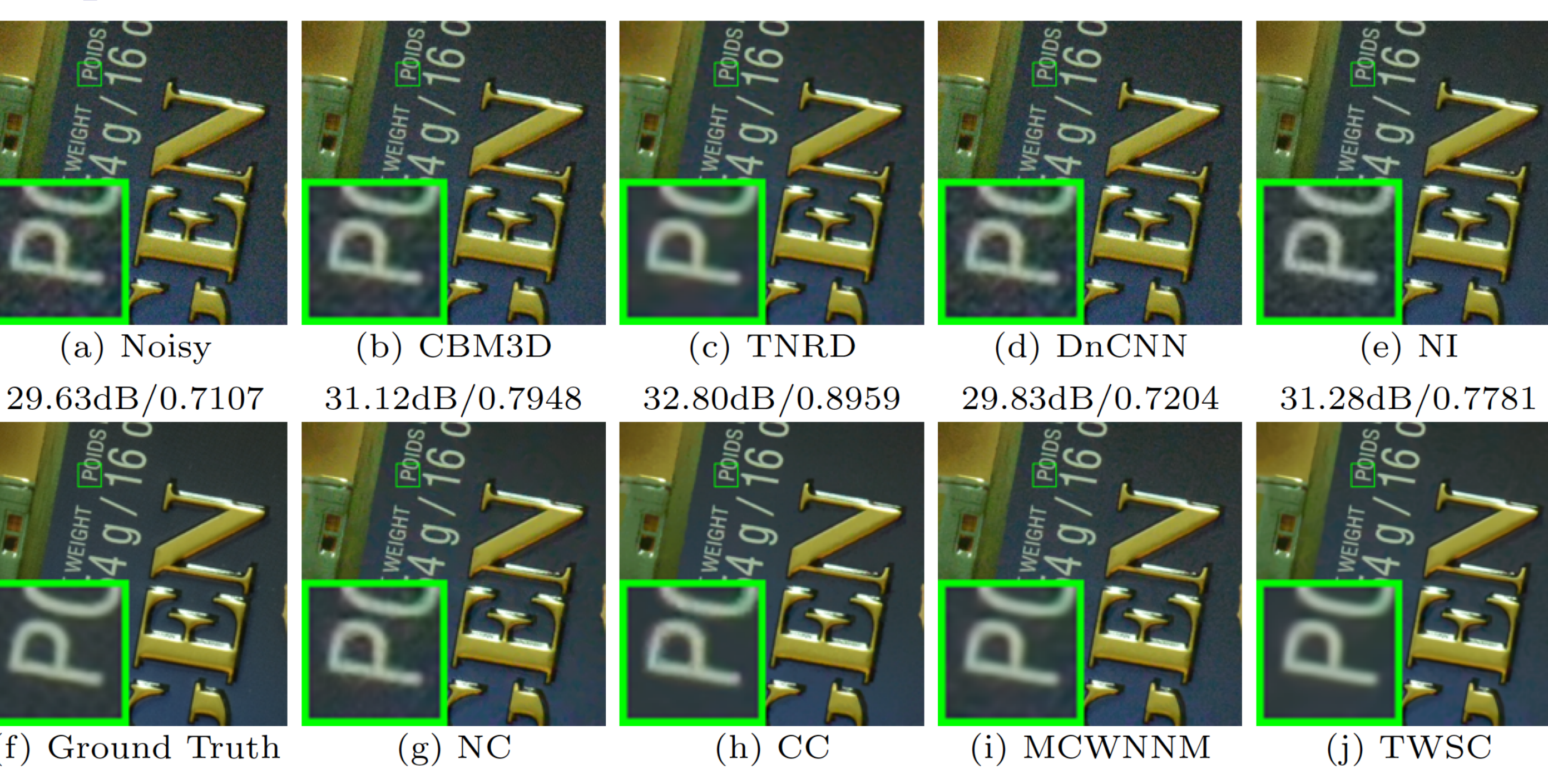
Table 3: Average results of PSNR(dB) and SSIM of different denoising methods on 1000 cropped real-world noisy images in [29].

	CBM3D	TNRD	DnCNN	NI	NC	MCWNNM	WSC	TWSC
PSNR	32.14	34.15	32.41	35.11	36.07	37.38	36.81	37.94
SSIM	0.7773	0.8271	0.7897	0.8778	0.9013	0.9294	0.9165	0.9403

Comparisons on Lena (AWGN with $\sigma = 75$):



Comparisons on Nikon D800 ISO 6400 1 in CC dataset [24]:

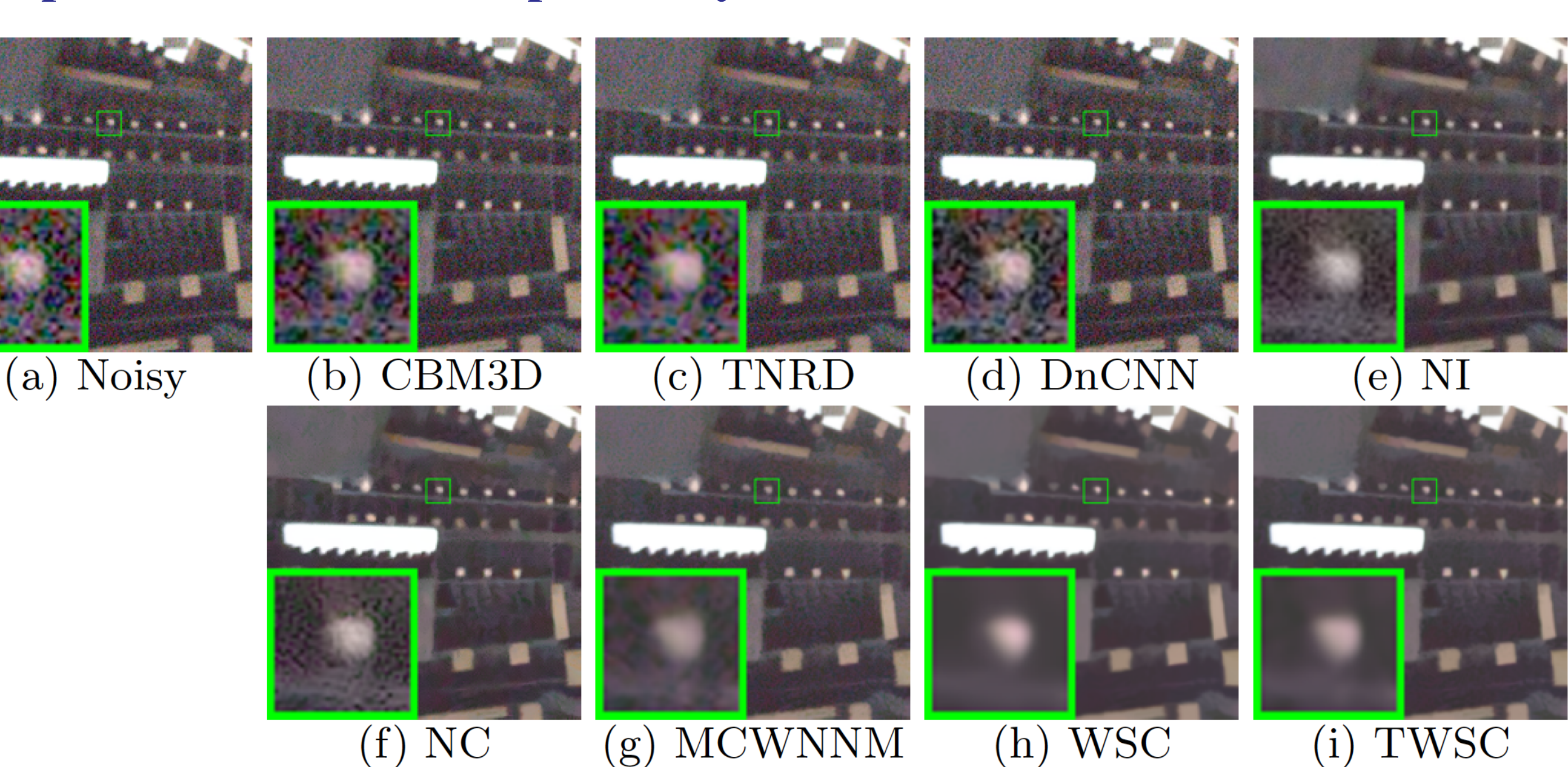


Quantitative Results on Speed:

Table 4: Average computational time (s) of different methods to process a 512×512 image in the DND dataset [29].

	CBM3D	TNRD	DnCNN	NI	NC	MCWNNM	WSC	TWSC
Time	6.9	5.2	79.5	1.1	15.6	208.1	188.6	195.2

Comparisons on 0001_2 captured by Nexus 6P in DND dataset [29]:



Github Webpage:

Code & Dataset

